ФИЗИКАЛЫҚ ҒЫЛЫМДАР
PHYSICAL SCIENCES
ФИЗИЧЕСКИЕ НАУКИ

UDC 53.03
IRSTI 29.03.45

https://doi.org/10.55452/1998-6688-2025-22-3-280-289

[1]Muratov M.M.,
PhD, Associate Professor, ORCID ID: 0000-0001-7270-9834,
e-mail: mukhit.muratov@gmail.com
[2]Zaitsev S.I.,
Dr.Phys.-Math.Sc., Professor, ORCID ID: 0000-0001-5120-8651,
e-mail: bachokg@gmail.com
[1]Pshikov M.I.,
PhD, Assistant Professor, ORCID ID: 0000-0002-6602-0018,
e-mail: mustahim.pshikov@gmail.com
[1]Guseinov N.R.,
Master's degree, ORCID ID: 0000-0003-4804-5323,
e-mail: solar_neo@mail.ru
[1]Nemkayeva R.R.,
Master's degree, ORCID ID: 0000-0002-8782-703X,
e-mail: quasisensus@mail.ru
[1]Mukhametkarimov Ye. S.,
PhD, Associate Professor, ORCID ID: 0000-0003-1381-4532,
e-mail: m.c.erzhan@mail.ru
[1]Tolepov Zh.K.,
PhD, ORCID ID: 0000-0001-7895-0434,
e-mail: mr.tolepov@mail.ru
[1]*Akhmetsadyk D.S.,
PhD student, ORCID ID: 0000-0003-2138-3314,
e-mail: d.akhmetsadyk@gmail.com

[1]Al-Farabi Kazakh National University, Almaty, Kazakhstan
[2]Institute of Microelectronics Technology and High Purity Materials RAS,
142432 Chernogolovka, Moscow region, Russia

DETERMINATION OF RESIST CONTRAST IN ELECTRON BEAM LITHOGRAPHY UNDER DEPTH-DEPENDENT NONUNIFORM ENERGY DEPOSITION

Abstract

The paper presents an analytical model for determining the resist contrast in electron lithography with nonuniform deposited energy over the depth, which is typical for low-energy electron exposure. In the classical

approach, the contrast is determined from the logarithmic dependence of the residual resist thickness on the exposure dose and assumes the homogeneity of the deposited energy over the layer depth, which leads to an overestimation of the contrast value in the presence of a gradient of the deposited energy. The proposed model takes into account the linear change in the energy profile in the resist, which is neglected in existing generally accepted model, thus allowing us to extract the "true" contrast value reflecting the resist properties under given development conditions. To validate the model, experiments were carried out with an ELP-20 resist 200 nm thick on silicon substrates at an electron beam energy of 5, 15 and 25 keV. Dose wedges were exposed for each energy, followed by development and topography analysis by atomic force microscopy. By fitting the model curves to the experimental dependence of the residual resist thickness on the exposure dose for each electron energy, the values of the contrast and the parameter characterizing the gradient of the deposited energy by depth were calculated. In this case, the contrast remains almost constant when varying the energy of incident electrons and has an average value of $\gamma = 1.67$. Thus, the increase in contrast with a decrease in the electron energy observed within the classical approach should be considered as an artifact of the model used. The proposed model is applicable for precision calibration of the processes of forming three-dimensional resist structures using the grayscale lithography.

Keywords: Electron beam lithography (EBL), Resist contrast, Nonuniform energy deposition, Analytical modeling, Grayscale lithography.

Introduction

Electron beam lithography is one of the most versatile and high-precision nanofabrication methods, widely used in such fields as micro- and nanoelectronics [1, 2], photonics [3] and plasmonics [4]. This method provides a resolution at the sub-10 nm level without the need for photomasks, which makes it an indispensable tool for creating integrated circuits [5], quantum devices [6] and nanostructures [7]. Despite its advantages, EBL has not received widespread use in mass production due to its relatively low productivity and high cost of equipment. However, it remains a key technology for prototyping [8], preparing samples for academic research [9], creating templates used in photolithography [10] and nanoimprint lithography [11]. Recently, special attention has been paid to the possibilities of three-dimensional structuring realized using grayscale EBL [12], in which modulation of the exposure dose allows the formation of continuous reliefs in the resist. This approach opens up prospects for the creation of complex phase plates [13, 14], photonic nanostructures and other functional 3D structures with micro- and nanometer accuracy [12, 15]. The implementation of such processes directly depends on the lithographic properties of the resists used, in particular their sensitivity and contrast, which are fundamental parameters determining the accuracy of creating a given profile, as well as the efficiency and resolution of the EBL processes. The sensitivity of the resist in EBL, determined by the minimum exposure dose required to completely remove the layer in a given development time, depends on the chemical composition of the resist, its molecular structure, layer thickness, incident electron energy and development time. In this case, a decrease in the incident electron energy, as a rule, leads to an increase in the sensitivity of the resist, which makes the low-energy EBL region (5–15 keV) especially attractive in terms of increasing the productivity of the process. This is due to the general physical principle: as the energy decreases, the interaction intensity increases. During exposure, the energy of penetrating electrons is spent on breaking molecular chains in the polymer matrix, which determines the rate of dissolution of the exposed resist in the developer. The resist contrast, reflecting the steepness of the transition from the undeveloped to the developed state, is determined not only by the molecular properties of the resist, but also by the exposure and development conditions, which significantly affect the clarity of the relief and the quality of the resulting structures. Knowledge of both parameters is critically important for both classical binary and grayscale EBL, especially when creating three-dimensional structures with high accuracy [16, 17]. It is generally accepted that under fixed conditions of resist formation and development, its contrast remains a value that does not depend on the energy of incident electrons. At the same time, the existing method for determining the resist contrast is to estimate the slope of the contrast curve [18] (the dependence of the residual resist thickness on the logarithm of the exposure dose). This approach is based on the assumption that the rate of resist dissolution is determined by the exposure dose according to a power law:

$$V \infty D^{\gamma} \quad (1)$$

where γ corresponds to the resist contrast. This is true in the case of electron exposure, when the penetration depth of the electron beam significantly exceeds the resist layer thickness, and the deposited energy is uniform across the resist thickness [16–19]. And since in real conditions there is always, albeit not always pronounced, a gradient of the deposited energy across the resist thickness, the determined contrast can be considered only a more or less effective estimate [20, 21]. However, at relatively low electron energies (5–15 keV) and films with a thickness of about 200 nm and higher, this assumption ceases to be valid, since the energy is deposited extremely nonuniformly across the layer thickness. This is due to a decrease in the penetration depth of electrons into the material and, thus, a shift in the maximum density of the absorbed energy to the surface, which leads to the formation of a pronounced gradient across the resist depth. As a result, such inhomogeneity leads to a significant distortion of the dose curve and, consequently, to a deviation of the measured contrast from the "true" value. At the same time, it is known from the results of numerical modeling of energy profiles using the Monte Carlo method that the growth of the deposited energy with depth can be approximated with good accuracy by a linear law [22, 23]. Based on this, relying on the existing development model and the results of Monte Carlo modeling, this paper proposes an analytical model for determining the "true" contrast of the electron resist under low-energy electron lithography conditions. The model is based on the assumption of a linear profile of the deposited energy with depth, which allows adjusting the contrast calculation taking into account the inhomogeneity of energy deposition with depth. This ensures obtaining a contrast value independent of the exposure conditions: electron energy and substrate material. This eliminates the contradiction between the overestimated contrast values obtained by the classical method and the "true" behavior of the resist, determined by its own properties under specific development conditions. The model also contains a parameter determined as a result of fitting, which characterizes the dose gradient by depth, i.e. the sensitivity of the dissolution rate to the inhomogeneity of the deposited energy. This parameter has both practical significance for optimizing development modes and scientific significance. The aim of this work is to develop a physically justified method for evaluating resist contrast that accounts for depth-dependent nonuniform energy deposition, thereby enabling the determination of the intrinsic (“true”) contrast of the resist, as opposed to the conventionally defined effective contrast.

Materials and methods

The substrate was a square of ~25×25 mm², cut with a diamond cutter from a standard silicon wafer of 100 mm diameter (orientation (111), n-type, thickness 500 μm, specific resistance 1–10 Ohm cm). Before use, it was cleaned in an ultrasonic bath: successively in acetone (purity 99.99%) and isopropyl alcohol (purity 99.8%), 10 minutes in each solution. The final stage of preparation was annealing at 200 °C for 5 minutes. The commercial positive resist ELP-20, intended for electron-beam lithography (JSC "NIOPIK"), was used as an electron-sensitive material, applied in the form of a 6% solution in chlorobenzene. The resist with a thickness of 200 nm was applied to the substrate by spin coating using an INSTRAS SCIENTIFIC spin coater in two stages: preliminary droplet spreading at 500 rpm for 5 seconds, followed by the main spin process at 3500 rpm for 60 seconds. After application, the resist films were subjected to heat treatment on a hot plate (FOUR E'S SCIENTIFIC) at 180°C for 15 minutes to remove residual solvent and impart the required hardness. Exposure of the resist with electrons was carried out on the basis of a Quanta 3D 200i (FEI company) scanning electron microscope under the control of the NanoMaker hardware and software complex, in the software environment of which structures were created and data for exposure were prepared. For the study of the resist sensitivity and contrast, a “dose wedge” test structure was used. It consisted of a sequential array of identical rectangles, each measuring 20 × 4 μm, with a total structure length of 84 μm. The exposure dose increased linearly from left to right along the wedge with a specified step within the required range. This approach made it possible to evaluate the dependence of the resist development on the received dose. Exposure was carried out at accelerating voltages of 5, 15, and 25 keV. After exposure, the samples were developed in a mixture of methyl isobutyl ketone (MIBK,

purity 99.0%) and isopropyl alcohol (IPA, purity 99.8%) in a ratio of 1:3 at a temperature of 25 °C for 20 seconds. Development was stopped by rinsing in deionized water for 5–10 seconds. The thickness of the resist film and the topography of the fabricated structures were studied by atomic force microscopy using a combined AFM-Raman Solver Spectrum system (NT-MDT, Russia) in the semi-contact scanning mode at a speed of 0.1 Hz to follow sharp thickness steps. NSG01 cantilevers from TipsNano with a tip curvature radius of less than 10 nm (resonance frequency ~170 kHz, typical stiffness 1.45–15.1 N/m) were used. Initial AFM scans with a typical scan area of 95 × 95 μm were processed in specialized Nova Px software, with data averaging performed over 10 profiles, and height profiles were constructed based on the processed data.

Proposed Method for Resist Contrast Determination

In positive resists, the primary mechanism responsible for the difference in solubility between exposed and unexposed regions is the radiation-induced scission of polymer chains [24, 25]. Irradiated chains, having a lower molecular weight, are less entangled and, accordingly, dissolve faster than unirradiated ones. The dependence of the dissolution rate V on the molecular weight M is described by a power law [25–28]:

$$V = cM^{-\gamma} \tag{2}$$

where c is a coefficient reflecting the amount of substance, and γ is the contrast [18]. The molecular weight M of the irradiated resist is inversely proportional to the average number of breaks in the polymer chain [29] and, therefore, is inversely proportional to the density of absorbed energy. This allows us to establish a relationship between the dissolution rate and the density of absorbed energy (ε):

$$\frac{V}{V_0} = \left(\frac{\varepsilon}{\varepsilon_0}\right)^{\gamma} \tag{3}$$

When measuring the contrast curve, relatively large (compared to the beam size) areas of the resist are exposed uniformly, then the etch depth is measured for each area at a given dose. Thus, the absorbed energy density can be considered as dependent only on the depth z and related to the exposure dose D by the expression:

$$\varepsilon(z) = \frac{D}{q} E_b \varepsilon_p(z) \tag{4}$$

where q is the electron charge, E_b is the electron energy, $\varepsilon_p(z)$ is the fraction of energy absorbed at depth z. The expression describing the fraction of deposited energy as a function of the resist depth during electron exposure was proposed based on the analysis of numerical modeling data presented in [22, 23], and has the following analytical form:

$$\varepsilon_p(z) = A(1 + az) \tag{5}$$

where a is a parameter that depends on the accelerating voltage and the nature of the substrate; A is the normalization coefficient.

The model based on equations (3)–(5) allows us to derive the dependence of the resist development depth h on the exposure dose D from the equation:

$$\int_0^{h(D)} \frac{dz}{(1+az)^{\gamma}} = const(D)^{\gamma} \tag{6}$$

Here const is a combination of the constants V_0, ε_0 and A. In practice, however, it is more convenient to use not the absolute etching depth, but the normalized remaining resist thickness H(D), defined as:

$$H(D) = 1 - \frac{h(D)}{h_0} \quad (7)$$

where h_0 is the initial resist thickness; for the full development (etching) of this thickness to the substrate, an exposure dose of D_0 is required. The contrast γ and the parameter a are restored by numerically fitting the theoretical dependence (7) to the experimental curve $H_{exp}(D)$, measured using atomic force microscopy.

Results and discussion

Figure 1 shows the experimental dose dependences of the ELP-20 resist thickness at different electron energies. The resist thickness is shown in relative units, and the dose axis is presented in a logarithmic scale. As can be seen from the presented data, with an increase in the electron energy, an increase in the dose required for complete development of the resist to the substrate is observed, since the value of this dose is determined by the specific energy losses of electrons in the material, described by the Bethe equation. In the energy range of 5–25 keV, and for a sufficiently thin resist, the specific energy losses of electrons in the resist can be considered inversely proportional to the energy of incident electrons – $dE/dx \propto 1/E$. In this case, the dose required to develop the resist to the substrate increases proportionally to the energy $D_0 \propto E$. This explains the quasi-linear increase in the dose D_0 with increasing electron energy observed in the experiment: at high energies, electrons lose less energy in the resist per unit length and penetrate deeper, which requires a higher dose to achieve an equivalent level of change as under low-energy conditions. The corresponding values of D_0 for different electron energies are given in Table 1.

The contrast calculation performed using the classical model according to [18, 27] is based on a quantitative analysis of the slope of the linear region of the dose curve on a logarithmic scale. The contrast γ* is defined as:

$$\gamma^* = tg(\theta^*) = \left| \frac{d\left(h/h_0\right)}{d\log_{10}\left(D/D_0\right)} \right| \quad (8)$$

where h is the residual resist thickness, h_0 is the initial thickness, D is the dose, D_0 is the dose required to develop the resist to the substrate (sensitivity). The contrast γ is related to γ* by the relation $\gamma = \gamma^*/\ln(10)$; the corresponding values are given in Table 1. As can be seen from the presented data, the contrast value increases with decreasing incident electron energy. Since all dose wedges were formed on the same substrate and developed under identical conditions, with the exception of the electron energy of the exposure beam, differences in the measured contrast values can be due to a change in the nature of energy deposition across the resist depth. Since the calculations were performed assuming a uniform energy distribution across the layer thickness, the obtained contrast values should be interpreted as effective, reflecting the combined effect of the dose gradient in the resist. Then, the contrast curves were fitted to the experimentally obtained dependences of the residual thickness on the exposure dose for different electron energies in accordance with formula (7). In addition to the contrast, the parameter a served as a fitting parameter. The fitting was performed individually for each energy, and in all cases the value of the determination coefficient R^2 (quantifying the fraction of the experimental data variance accounted for by the model) exceeded 0.97. The results of fitting the model curve to the experimental dependence of the residual resist thickness on the dose for different electron energies are given in Table 1. As can be seen, the calculations performed on the basis of the proposed model give an average contrast value of $\gamma = 1.67$. In addition, at high energies of incident electrons, the contrast values obtained both in the classical approximation and within the framework of the proposed model converge to the same limiting value.

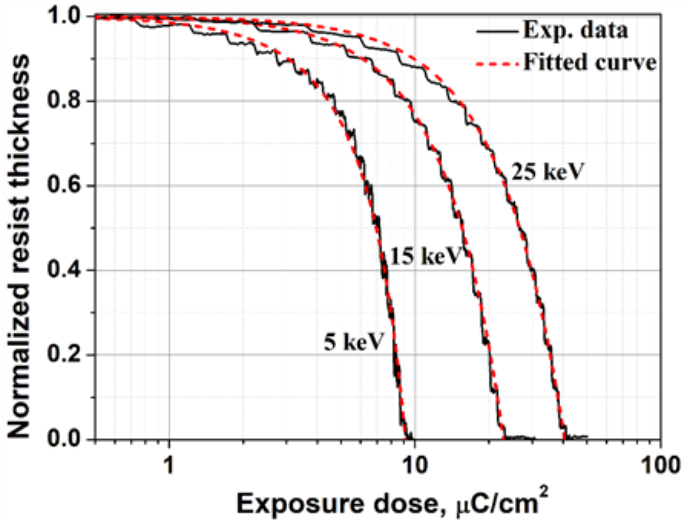

Figure 1 – Dependence of the residual thickness of ELP-20 resist on the exposure dose at electron energies of 5, 15, and 25 keV. The model curves were obtained by parametric fitting to the experimental data using the proposed approach

Table 1 – Lithographic parameters of the ELP-20 resist determined as a function of electron energy. For comparison, the values calculated using the classical model (γ_{eff}) and the model proposed in this work (γ) are presented

	Electron beam energy (in keV)		
Lithographic parameters	5	15	25
D_0, μC/cm^2	9.1	22.8	41.2
γ_{eff}	2.61	1.85	1.65
γ	1.69	1.65	1.67
a, (10^{-3} nm^{-1})	3.55	0.45	0.10

The behavior of the parameter a, which characterizes the gradient of the deposited energy, deserves special attention in Table 1. Its sharp decrease with increasing energy (from 3.55×10^{-3} nm^{-1} at 5 keV to 0.10×10^{-3} nm^{-1} at 25 keV) reflects a physically justified weakening of the inhomogeneity of the energy profile. This behavior is generally consistent with the calculations performed by the Monte Carlo method in [22, 23] and indicates an increase in the density of the deposited energy from the surface to the substrate, which is especially pronounced with a decrease in the electron beam energy. The exact degree of agreement depends on the chosen calculation model, including the description of the braking and the parameters of the interaction of electrons with matter. For the case of 5 keV energy and resist thickness h_0=200 nm, with gradient coefficient $a=3.55\times10^{-3}$ nm^{-1}, the value of the product $ah_0 \approx 0.71$, according to expression (5), ah_0 shows a pronounced increase in the deposited dose from the surface to the substrate and the ratio of the absorbed energy values at z=0 and z=h_0 is 1.71. In contrast, at 25 keV energy, the value $ah_0 \approx 0.02$, which indicates a virtually uniform dose distribution across the layer thickness. Thus, the introduced parameter a has not only an adjustable meaning, but also a physical interpretation, characterizing the degree of exposure inhomogeneity.

Conclusion

A 200 nm thick ELP-20 resist layer on a silicon substrate was exposed using low-energy electrons in the range of 5–25 keV. The deposited dose distribution was modeled using a semi-analytical approach, assuming a linear increase in absorbed energy density with depth, which is consistent with Monte Carlo simulation results. The resist contrast was determined by numerically fitting the development depth as a function of dose, taking into account the dose gradient characterized by the parameter a. This approach eliminates the contrast overestimation inherent in the classical model, which assumes uniform energy deposition. It was shown that the true resist contrast remains nearly constant with varying energy $\gamma \approx 1.67$, whereas the effective contrast γ_{eff} increases from 1.65 to 2.61 as the energy decreases, due to the nonuniform dose distribution. The dose required for complete development increases quasi-linear from 9.1 to 41.2 μC/cm², in accordance with the dependence $-dE/dx \propto 1/E$. The parameter a, reflecting the degree of the dose gradient, decreases from 3.55×10^{-3} to 0.10×10^{-3} nm^{-1} with increasing energy, indicating a reduction in the inhomogeneity of the deposition profile. The developed model is a physically grounded method for contrast determination, suitable for three-dimensional resist structuring using grayscale lithography. It eliminates the influence of exposure parameters and substrate properties, extends the classical approach to contrast evaluation, and is easily integrated into standard dose-response analysis techniques.

Acknowledgments

This research was carried out with financial support from the Committee of Science of the Ministry of Science and Higher Education of the Republic of Kazakhstan (Grant No. AP19576960).

REFERENCES

1 Flodgren, V., Das, A., Sestoft, J.E., Löfström, N., Alcer, D., Jeddi, H., Borgström, M.T., Pettersson, H., Nygård J. and Mikkelsen A. Flexible fabrication of aligned multi-nanowire circuits for on-chip prototyping. Microelectronic Engineering, 300, article 112363 (2025). https://doi.org/10.1016/j.mee.2025.112363.

2 Pan, Y. and Xu, K. Recent progress in nano-electronic devices based on EBL and IBL. Current Nanoscience, 16 (2), 157–169 (2020). https://doi.org/10.2174/1573413715666190701111638.

3 Sahoo, P.K., Coates, E., Silver, C.D., Li, K., and Krauss, T.F On the reproducibility of electron-beam lithographic fabrication of photonic nanostructures. Scientific Reports, 14, article 8703 (2024). https://doi.org/10.1038/s41598-024-58842-w.

4 Chen, Y., Zhang, H., Zhang, Z., Zhu, X., and Fang, Z. Dual views of plasmonics: from near-field optics to electron nanoscopy. Photonics Insights, 4 (2), article R04 (2025). https://doi.org/10.3788/PI.2025.R04.

5 Bakar, R.A., Hassan, H., and Herman, S.H. Patterning of monolithic integrated circuit using electron beam lithography. Proc. of the 2023 IEEE 13th International Conf. on System Engineering and Technology (ICSET), (Shah Alam, Malaysia, 2 October, 2023), pp. 319–323. https://doi.org/10.1109/ICSET59111.2023.10295127.

6 Ko, T., Kumar, S., Shin, S., Seo, D., and Seo, S. Colloidal quantum dot nanolithography: direct patterning via electron beam lithography. Nanomaterials, 13 (14), article 2111 (2023). https://doi.org/10.3390/nano13142111.

7 Chen, Y. Nanofabrication by electron beam lithography and its applications: a review. Microelectronic Engineering, 135, 57–72 (2015). https://doi.org/10.1016/j.mee.2015.02.042.

8 Yasar, F., Muller, R.E., Khoshakhlagh, A., and Keo, S.A. Large-area fabrication of nanometer-scale features on GaN using e-beam lithography. Journal of Vacuum Science & Technology B, 42, article 022801 (2024). https://doi.org/10.1116/6.0003270.

9 Zheng, X., Calò, A., Albisetti, E., et al. Patterning metal contacts on monolayer MoS_2 with vanishing Schottky barriers using thermal nanolithography. Nature Electronics, 2, 17–25 (2019). https://doi.org/10.1038/s41928-018-0191-0.

10 Hudek, P., Jurkovic, M., Choleva, P., Wroczewski, W., Hashimoto, M., Ono, K., Fukui, T., Takahashi, T., and Takahashi, K. Multi-beam mask writer exposure optimization for EUV mask stacks. Journal of Micro/Nanopatterning, Materials, and Metrology, 20 (4), article 041402 (2021). https://doi.org/10.1117/1.JMM.20.4.041402.

11 Baracu, A.M., Avram, M.A., Breazu, C., Bunea, M.-C., Socol, M., Stanculescu, A., Matei, E., Thrane, P.C.V., Dirdal, C.A., Dinescu A. and Rasoga O. Silicon metalens fabrication from electron beam to UV-nanoimprint lithography. Nanomaterials, 11 (9), article 2329 (2021). https://doi.org/10.3390/nano11092329.

12 Khonina, S.N., Kazanskiy, N.L., and Butt, M.A. Grayscale lithography and a brief introduction to other widely used lithographic methods: a state-of-the-art review. Micromachines, 15 (11), article 1321 (2024). https://doi.org/10.3390/mi15111321.

13 Massari, M., Ruffato, G., Gintoli, M., Ricci, F., and Romanato, F. Fabrication and characterization of high-quality spiral phase plates for optical applications. Applied Optics, 54 (13), 4077–4083 (2015). https://doi.org/10.1364/AO.54.004077.

14 Grushina, A. Direct-write grayscale lithography. Advanced Optical Technologies, 8 (3–4), 163–169 (2019). https://doi.org/10.1515/aot-2019-0024.

15 Li, K., Li, J., Reardon, C., Schuster, C.S., Wang, Y., Triggs, G.J., Damnik, N., Müenchenberger, J., Wang, X., Martins, E.R., and Krauss, T.F. High speed e-beam writing for large area photonic nanostructures – a choice of parameters. Scientific Reports, 6, article 32945 (2016). https://doi.org/10.1038/srep32945.

16 Zaitsev, S., Knyazev, M., Dubonos, S., and Bazhenov, A. Fabrication of 3D photonic structures. Microelectronic Engineering, 73–74, 383–387 (2004). https://doi.org/10.1016/j.mee.2004.02.074.

17 Svintsov, A.A., Knyazev, M.A., and Zaitsev, S.I. Calculation of the absorbed electron energy 3D distribution by the Monte Carlo method, presentation of the proximity function by three parameters α, β, η and comparison with the experiment. Materials, 15, article 3888 (2022). https://doi.org/10.3390/mi14112060.

18 Knyazev, M.A., Dubonos, S.V., Svintsov, A.A., and Zaitsev, S.I. Fast electron resist contrast determination by “fitting before measurement” approach. Microelectronic Engineering, 84 (5–8), 1080–1083 (2007). https://doi.org/10.1016/j.mee.2007.01.145.

19 Myrzabekova, M.M., Guseinov, N.R., Zaitsev, S.I., Shabelnikova, Ya.L., Muratov, M.M., Muradova, S.R., and Turarbaeva, T.B. Study of the electron lithography parameters by AFM. Recent Contributions to Physics, 68 (1), 81–90 (2019). https://doi.org/10.26577/RCPh-2019-1-1112.

20 Gangnaik, A.S., Georgiev, Y.M., and Holmes, J.D. New Generation Electron Beam Resists: A Review. Chemistry of Materials, 29 (5) (2017). https://doi.org/10.1021/acs.chemmater.6b03483.

21 Jin, Y., Moreno, M., Vianez, P.M.T., Tan, W.K., Griffiths, J.P., Farrer, I., Ritchie, D.A., and Ford, C.J.B. Microscopic metallic air-bridge arrays for connecting quantum devices. Applied Physics Letters, 118, article 162108 (2021).https://doi.org/10.1063/5.0045557.

22 Rogozhin, A.E., and Sidorov, F.A. E-beam lithography simulation techniques. Russian Microelectronics, 49 (2), 108–122 (2020). https://doi.org/10.1134/S1063739720010096.

23 Tabata, T. Theoretical evaluation of absorbed doses in materials irradiated by low-energy electron beams: a short review. Bulletin of University of Osaka Prefecture, Series A, 44 (1), 41–46 (1995). https://doi.org/10.24729/00008333.

24 Ed. P.W. Hawkes, Advances in Imaging and Electron Physics (Academic Press, 1998).

25 Ed. P. Rai-Choudhury, Handbook of Microlithography, Micromachining and Microfabrication, Chapter 2 (SPIE, 1997).

26 Asmussen, F., and Ueberreiter, K. Velocity of dissolution of polymers. Part II. Journal of Polymer Science, 57, 199–208 (1962). https://doi.org/10.1002/pol.1962.1205716516.

27 Bernstein, G.H., Hill, D.A., and Liu, W.-P. New high-contrast developers for poly(methyl methacrylate) resist. Journal of Applied Physics, 71, 4066–4075 (1992). https://doi.org/10.1063/1.350831.

28 Moreau, W.M. Semiconductor Lithography: Principles, Practices, and Materials (Springer Science & Business Media, 2012).

29 Moreau, W.M. Semiconductor Lithography: Principles, Practices, and Materials, part II (Mir, 1990, in Russ.).

[1]Муратов М.М.,
PhD, қауымдастырылған профессор, доцент, ORCID ID: 0000-0001-7270-9834,
e-mail: mukhit.muratov@gmail.com
[2]Зайцев С.И.,
ф.-м.ғ.д., профессор, ORCID ID: 0000-0001-5120-8651,
e-mail: bachokg@gmail.com
[1]Пшиков М.И.,
PhD, ассистент-профессор, ORCID ID: 0000-0002-6602-0018,
e-mail: mustahim.pshikov@gmail.com
[1]Гусейнов Н.Р.,
магистр, ORCID ID: 0000-0003-4804-5323,
e-mail: solar_neo@mail.ru
[1]Немкаева Р.Р.,
магистр, ORCID ID: 0000-0002-8782-703X,
e-mail: quasisensus@mail.ru
[1]Мухаметкаримов Е.С.,
PhD, қауымдастырылған профессор, доцент, ORCID ID: 0000-0003-1381-4532,
e-mail: m.c.erzhan@mail.ru
[1]Төлепов Ж.Қ.,
PhD, ORCID ID: 0000-0001-7895-0434,
e-mail: mr.tolepov@mail.ru
[1]*Ахметсадык Д.С.,
докторант, ORCID ID: 0000-0003-2138-3314,
*e-mail: d.akhmetsadyk@gmail.com

[1]Әл-Фараби атындағы Қазақ ұлттық университеті, Алматы қ., Қазақстан
[2]Микроэлектроника технологиясы және жоғары тазалықтағы материалдар институты РҒА, Черноголовка, Мәскеу облысы, Ресей

ТЕРЕҢДІК БОЙЫМЕН ЭНЕРГИЯНЫҢ БІРКЕЛКІ БӨЛІНБЕУІ ЖАҒДАЙЫНДА ЭЛЕКТРОНДЫ-СӘУЛЕЛІК ЛИТОГРАФИЯДАҒЫ РЕЗИСТ КОНТРАСТЫН АНЫҚТАУ

Аңдатпа

Бұл жұмыста төмен энергиялы электрондық сәулемен экспонирлеу кезінде тереңдік бойымен энергияның біркелкі емес тұнуына тән жағдайларда резистің контрастын анықтауға арналған аналитикалық модель ұсынылған. Классикалық әдісте контраст экспонирлеу дозасына қатысты резистің қалдық қалыңдығының логарифмдік тәуелділігі арқылы анықталады және энергияның қабат тереңдігі бойынша біркелкі тұнады деп қарастырылады, бұл энергияның градиенті болған жағдайда контраст мәнін асыра бағалауға әкеледі. Ұсынылған модель резистегі энергия профилінің сызықты өзгерісін ескеруге мүмкіндік береді, осылайша берілген өңдеу жағдайларында резистің шынайы қасиеттерін бейнелейтін «нақты» контраст мәнін алуға жол ашады. Модельді тексеру мақсатында 5, 15 және 25 кэВ энергиялы электрондар шоғырымен кремний төсеніштеріне отырғызылған 200 нм қалыңдықтағы ЭЛП-20 резисті сынақтан өткізілді. Әрбір энергия үшін дозалық сынамалар экспонирленіп, кейін өңделіп, топографиясы атомдық-күштік микроскопия әдісімен зерттелді. Резистің қалдық қалыңдығының дозаға тәуелді эксперименттік деректеріне модельдік қисықтарды сәйкестендіру арқылы әрбір энергия үшін контраст мәндері және тереңдік бойымен энергия тұну градиентін сипаттайтын параметр есептелді. Нәтижесінде, электрондар энергиясы өзгергенімен контраст шамамен тұрақты болып қалып, орташа мәні $\gamma = 1.67$ болды. Осылайша, классикалық әдіс бойынша энергия төмендеген сайын байқалатын контрастың артуы модель артефактісі ретінде қарастырылуы тиіс. Ұсынылған модель сұр реңді литография әдісімен үш өлшемді резистік құрылымдарды дәл қалыптастыру процестерін калибрлеу үшін қолдануға жарамды.

Тірек сөздер: электронды-сәулелік литография, резист контрасты, тереңдік бойымен энергияның біркелкі емес тұнуы, аналитикалық модель, сұр реңді литография.

[1]Муратов М.М.,
PhD, ассоциированный профессор, доцент, ORCID ID: 0000-0001-7270-9834,
e-mail: mukhit.muratov@gmail.com
[2]Зайцев С.И.,
д.ф.-м.н., профессор, ORCID ID: 0000-0001-5120-8651,
e-mail: bachokg@gmail.com
[1]Пшиков М.И.,
PhD, ассистент-профессор, ORCID ID: 0000-0002-6602-0018,
e-mail: mustahim.pshikov@gmail.com
[1]Гусейнов Н.Р.,
магистр, ORCID ID: 0000-0003-4804-5323,
e-mail: solar_neo@mail.ru
[1]Немкаева Р.Р.,
магистр, ORCID ID: 0000-0002-8782-703X,
e-mail: quasisensus@mail.ru
[1]Мухаметкаримов Е.С.,
PhD, ассоциированный профессор, доцент, ORCID ID: 0000-0003-1381-4532,
e-mail: m.c.erzhan@mail.ru
[1]Толепов Ж.К.,
PhD, ORCID ID: 0000-0001-7895-0434,
e-mail: mr.tolepov@mail.ru
[1]*Ахметсадык Д.С.,
докторант, ORCID ID: 0000-0003-2138-3314,
*e-mail: d.akhmetsadyk@gmail.com

[1]Казахский национальный университет им. аль-Фараби, г. Алматы, Казахстан
[2]Институт проблем технологии микроэлектроники и особо чистых материалов РАН,
г. Черноголовка, Московская область, Россия

ОПРЕДЕЛЕНИЕ КОНТРАСТА РЕЗИСТА В ЭЛЕКТРОННО-ЛУЧЕВОЙ ЛИТОГРАФИИ ПРИ НЕОДНОРОДНО ОСАЖДЕННОЙ ЭНЕРГИИ ПО ГЛУБИНЕ

Аннотация

В работе представлена аналитическая модель определения контраста резиста в электронной литографии при неоднородно осажденной энергии по глубине, что характерно для низкоэнергетического электронного экспонирования. В классическом подходе контраст определяется из логарифмической зависимости остаточной толщины резиста от дозы экспонирования и предполагает однородность осажденной энергии по глубине слоя, что приводит к переоценке значения контраста при наличии градиента осажденной энергии. Предлагаемая модель учитывает в существующей модели линейное изменение энергетического профиля в резисте, позволяя извлечь «истинное» значение контраста, отражающее свойства резиста при заданных условиях проявления. Для валидации модели были проведены эксперименты с резистом ЭЛП-20 толщиной 200 нм на кремниевых подложках при энергии электронов в пучке 5, 15 и 25 кэВ. Дозовые клинья экспонировались для каждой энергии с последующим проявлением и анализом топографии методом атомно-силовой микроскопии. Путем подгонки модельных кривых к экспериментальной зависимости остаточной толщины резиста от дозы экспонирования для каждой энергии электронов были рассчитаны значения контраста и параметра, характеризующего градиент осажденной энергии по глубине. При этом контраст остается практически постоянным при варьировании энергии падающих электронов и имеет среднее значение $\gamma = 1.67$. Таким образом, увеличение контраста при уменьшении энергии электронов, наблюдаемое в рамках классического подхода, следует рассматривать как артефакт используемой модели. Предложенная модель применима для прецизионной калибровки процессов формирования трехмерных резистных структур методом литографии серого тона.

Ключевые слова: электронно-лучевая литография, контраст резиста, неоднородное осаждение энергии по глубине, аналитическая модель, литография серого тона.

Article submission date: 17.07.2025